# REVIEW

CHEMISTRY

Special Topic: Aggregation-Induced Emission

# Molecular design and application of luminescent materials composed of group 13 elements with an aggregation-induced emission property

Shunichiro Ito ⓘD, Masayuki Gon, Kazuo Tanaka* and Yoshiki Chujo

## ABSTRACT

Complexation of $\pi$-conjugated ligands by metal or semimetal ions leads to the enhancement of the planarity and rigidity of $\pi$-conjugated systems. Boron, especially, has played a central role in the design of luminescent main-group complexes. However, these complexes still suffer the disadvantage of aggregation-caused quenching as well as typical organic fluorophores. It has recently been reported that some types of boron complexes exhibit the aggregation-induced emission (AIE) property. Moreover, AIE behavior from complexes and organometallic compounds composed of the other group 13 elements, such as aluminum and gallium, has emerged in this decade. These observations greatly encourage us to develop advanced functional materials based on the group 13 elements. Indeed, recent research has demonstrated that these classes of materials are potentially versatile scaffolds for constructing chromic luminophores, efficiently emissive $\pi$-conjugated polymers and so on. This review mainly describes AIE-active group 13 complexes with four-coordinate structures and their application as photo-functional materials. Proposed mechanisms of the origins of AIE behavior are briefly discussed.

**Keywords:** aggregation-induced emission, crystallization-induced emission, chromism, conjugated polymer, group 13

Department of Polymer Chemistry, Graduate School of Engineering, Kyoto University, Kyoto 615-8510, Japan

*Corresponding author. E-mail: tanaka@poly.synchem.kyoto-u.ac.jp

## INTRODUCTION

To obtain optimal luminescent properties from organic compounds, chemists have developed various types of $\pi$-conjugated compounds over the last 150 years, such as polyaromatic hydrocarbons [1–3], cyanines [4–6], coumarins [7], etc. These luminescent molecules with superior properties possess rigid, planar and often large $\pi$-conjugated electronic systems. Such structures generally lead to strong coloration and efficient photoluminescence. In this context, the complexation of $\pi$-conjugated ligands with metal or semimetal elements has recently been utilized to construct highly emissive molecules. $\pi$-Conjugated ligands locked by coordination bonds result in efficient luminescence in many cases because the complexation enhances molecular rigidity, planarity and effective $\pi$-conjugation length. For instance, $4'$-difluoro-4-bora-3a,4a-*s*-indacene (BODIPY) and its derivatives, whose dipyrrin ligands can be regarded as a substructure of porphyrins (Fig. 1), exhibit strong absorption and extraordinarily high fluorescence quantum yields in the solution state. BODIPY dyes also exhibit many superb properties, e.g. redox activity, electron transfer and near-infrared emission [8,9].

However, these classes of luminescent dyes often face a severe problem in that many of these complexes lose their emission in the solid or concentrated states due to self-absorption and intermolecular interactions, which give rise to the formation of non-luminescent excitonic states. Such a phenomenon is known as concentration quenching or aggregation-caused quenching (ACQ). The planar structures of the complexes derived from the complexation cause this drawback, although such
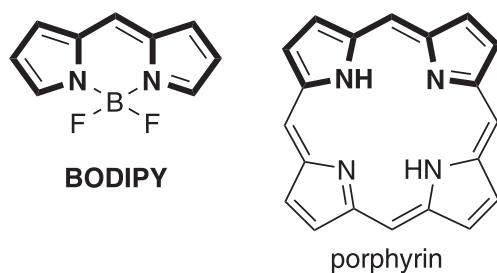
**Figure 1.** The chemical structure of BODIPY and porphyrin. The common structure is emphasized.

structural features play a pivotal role in achieving the splendid emission properties. When luminescent materials are applied to anti-counterfeit inks, film-type sensors, light-emitting diodes or other situations requiring a high concentration of dyes, they need to emit efficiently in the concentrated or solid states. Therefore, the trade-off between the complexation and the solid-state luminescence should be circumvented.

Since the aggregation-induced emission (AIE) effect was conceptualized for siloles and tetraphenylethenes, many types of AIE-active compounds have been reported [10–12]. Most of the AIE-active molecules contain bulky and movable substituents, such as phenyl groups, attached to their chromophoric $\pi$-systems. These substituents consume excited energy through radiationless processes in the solution states, for example, molecular motions or vibrations. These non-luminescent processes can be suppressed by structural restriction in the concentrated states. The substituents also restrict undesired intermolecular interactions leading to the formation of dark states. Thus, the aggregated AIE-active dyes emit more efficiently than the diluted ones. This significant concept of AIE has shed new light on the molecular design strategy of luminescent boron complexes as well as purely organic luminophores. Indeed, growing numbers of boron-containing molecules and polymers with AIE behavior have been reported over the last decade [12–15]. In addition, some complexes show a crystallization-induced emission (CIE) property. The crystals of CIE-active materials exhibit higher photoluminescence quantum yields than both their amorphous solids and their dilute solutions. Utilizing these classes of compounds, many researchers have developed stimuli-responsive materials, luminescent sensors, emissive films based on AIE-active polymers and so on. Moreover, some examples of the AIE- and CIE-active compounds containing aluminum or gallium have also been explored gradually.

Heteroatoms, including not only nonmetals but also semimetals, typical, and transition metals, often serve as a key to functionalizing both small
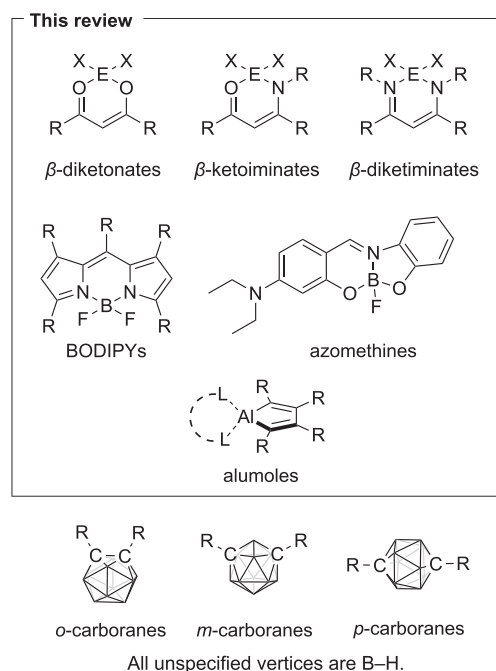


**Figure 2.** Chemical structures of various scaffolds of AIE-active materials composed of group 13 elements (E = B, Al or Ga; R = aryl, alkyl etc.; X = halogen, aryl etc.).

molecules and polymers thanks to the promising electronic nature of these atoms. In this context, advanced functional materials can be achieved in a bottom-up manner by elaborately designing a minimal functional unit using heteroatoms. We have regarded such a minimal functional unit as an 'element block' [13–15]. Based on this idea, it has been discovered that various types of boron complexes and cluster compounds work as versatile element blocks for realizing AIE behavior. This review mainly focuses on four-coordinate complexes of group 13 elements with AIE and/or CIE properties (Fig. 2). In addition to the coordination compounds, carboranes, which are cluster compounds composed of 10 boron and two carbon atoms, are also known to be a scaffold for AIE-gens. Carborane-based systems have been covered in recent comprehensive reviews [12,16] and will not be mentioned.

## BORON-CONTAINING COMPOUNDS

Four-coordinate boron complexes are usually more stable with regard to air and water than three-coordinate ones because the 2p orbitals of four-coordinated boron are no longer vacant [17]. Consequently, four-coordinate boron complexes have been most extensively investigated in the chemistry of the AIE behavior of boron-containing molecules. Most studies mainly focus on the development of new chelate ligands for obtaining the AIE property, and the effects of substituents
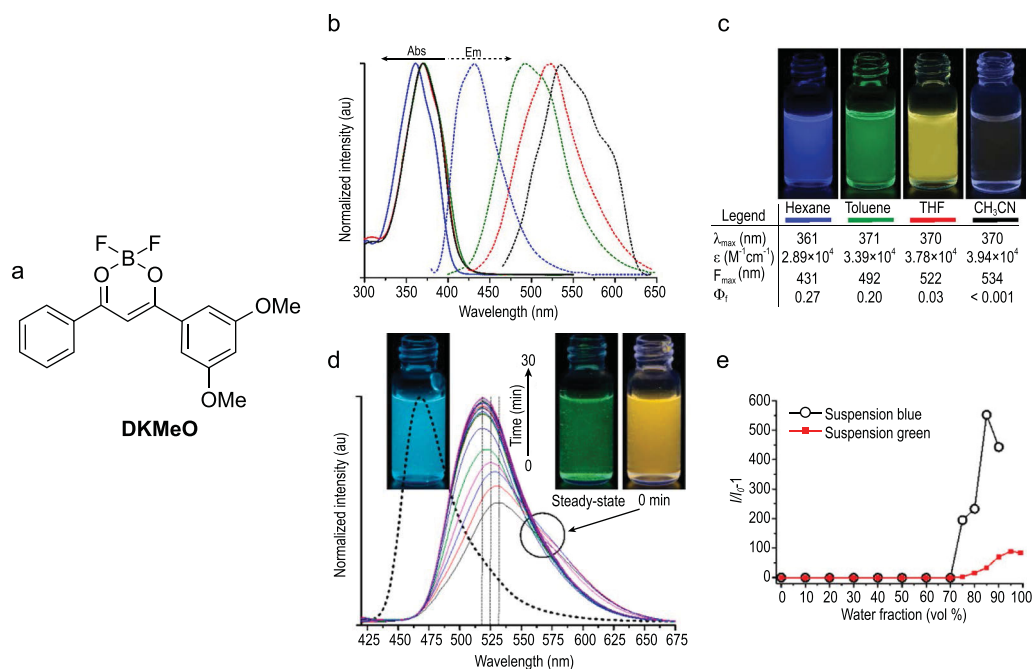
**Figure 3.** (a) The chemical structure of the AIE-active $\beta$-diketonate boron complex. (b) Photoelectronic spectra of DKMeO in various solvents. (c) Photographic images of DKMeO in hexane, toluene, tetrahydrofuran (THF) and acetonitrile under UV irradiation. (d) Photoluminescence spectra of blue suspension (dotted line) and time-dependent spectra of green suspension (solid lines) in $5 \times 10^{-5}$ M CH$_3$CN/water mixture at 85% and 95% fraction of water ($f_w$), respectively. (e) A plot of relative luminescent intensity versus $f_w$. $I_0$ represents emission intensity in pure $5 \times 10^{-5}$ M CH$_3$CN solution. Reprinted with permission from ref [23]. Copyright 2014 American Chemical Society.

on photophysical properties, such as AIE activity, luminescent color and stimuli responsivity. This section will describe typical examples of AIE- or CIE-active four-coordinate boron complexes and discuss proposed origins of the AIE nature of this class of materials.

## Boron $\beta$-diketonate complexes

$\beta$-Diketonates are one of the most widely utilized ligands for obtaining metal complexes with various metal ions. Boron $\beta$-diketonates are known to be versatile units for obtaining luminescent materials including polymers because of their superior luminescent properties e.g. mechanochromism, thermochromism and room-temperature phosphorescence [18–22]. However, the ACQ problem is inevitable for most of this class of complex because of their relatively planar structures resulting in undesired intermolecular interactions. Nevertheless, the AIE property has been obtained from several boron $\beta$-diketonates [23,24].

Fascinating photophysical properties were observed in dimethoxy-substituted $\beta$-diketonate boron complex DKMeO (Fig. 3) [23]. The luminescence from this compound showed not only an AIE property but also dependence on polymorphs, mechanochromism, thermochromism and solva-

tochromism. DKMeO exhibited a slight emission in the acetonitrile solution ($\Phi_f < 0.001$, Fig. 3c), while the complex emitted much more strongly after the addition of an excess amount of water to form aggregates. Interestingly, the luminescent color was dependent on the way of adding water even if the final volume content of water was the same. When water was added dropwise to the vigorously stirred acetonitrile solutions, the obtained suspensions showed blue emission. On the other hand, the emission color was dramatically changed from yellow to green when the whole amount of water was added at once to prepare acetonitrile/water mixtures (Fig. 3d). The results of powder X-ray diffraction patterns and photophysical measurements showed that the blue and green emissions originated from the two distinct polymorphs, which are derived from the *syn–anti* conformers of the methoxy groups. The transient yellow-emissive suspension might be attributed to the metastable amorphous state. It should be noted that DKMeO showed relatively efficient emission in the less polar solvents (hexane, toluene and tetrahydrofuran), as shown in Fig. 3b and c. Therefore, the mechanism of the AIE phenomenon might not only be the restriction of the molecular motion but also the difference of polarity between the solution and aggregate states. By clarifying the reason why the molecular

crystals of this compound are spared the problem of ACQ, far more sophisticated molecular designs are expected to be established for obtaining AIE-active materials based on $\beta$-diketonate complexes.

## Boron $\beta$-ketoiminate complexes

As mentioned above, $\beta$-diketonate is still not a robust structure as a scaffold of AIE-active luminophores. In contrast, it has been shown that $\beta$-ketoiminate ligands, also denoted as $\beta$-iminoenolates or $\beta$-enaminoketonates, are a versatile scaffold for the construction of AIE-gens [25–33]. $\beta$-Ketoiminate skeletons are the imine analogues of $\beta$-diketonate ligands, and the nitrogen atom is substituted by aryl, alkyl, silyl etc. In general, B–N bonds ($\sim$445.6 kJ mol$^{-1}$ or less) are weaker than B–O bonds ($\sim$536 kJ mol$^{-1}$) [34]. The weaker bond energy is likely to result in larger molecular motions both at the ground and excited states. Therefore, non-radiative quenching processes of the corresponding boron complexes in the solution states are probably accelerated by the replacement of oxygen to nitrogen. In solid states, such molecular motions would be restricted, and the steric hinderance of the substituent attached to the nitrogen atoms could contribute to prohibiting strong intermolecular interaction. Consequently, it could be hypothesized that boron $\beta$-ketoiminate complexes are likely to emit more efficiently in solid states than those in solution states.

AIE-active boron $\beta$-ketoiminates have been synthesized with various types of ligands [25–33]. A typical example is shown in Fig. 4 [26]. The solid of $\beta$-diketonate complex BDK exhibited a decrease in photoluminescence intensity and quantum yield ($\Phi_{PL} = 0.36$) compared to those of the solution ($\Phi_{PL} = 0.91$). On the other hand, the corresponding boron $\beta$-ketoiminates, BKIa, BKIb and BKIc, showed drastic emission enhancement caused by aggregation ($\Phi_{PL}^{solid}$: 0.76 for BKIa; 0.42 for BKIb; 0.30 for BKIc), while the emissions from their solution samples were very weak ($\Phi_{PL}^{solution} \sim 0.01$). Under frozen and viscose conditions, the emission intensity of these complexes increased compared to that in the solutions. These results support that intramolecular motions should accelerate non-radiative quenching paths in solution at room temperature.

Since AIE-active boron $\beta$-ketoiminates have relatively high planarity, it is expected that the extension of the $\pi$-electronic planes could effectively modulate their photophysical properties. Mechanical stimuli, such as pressing, crushing and grinding, occasionally change the luminescent color of crystalline samples of solid-state emissive molecules. This property is called mechano- or piezochromic
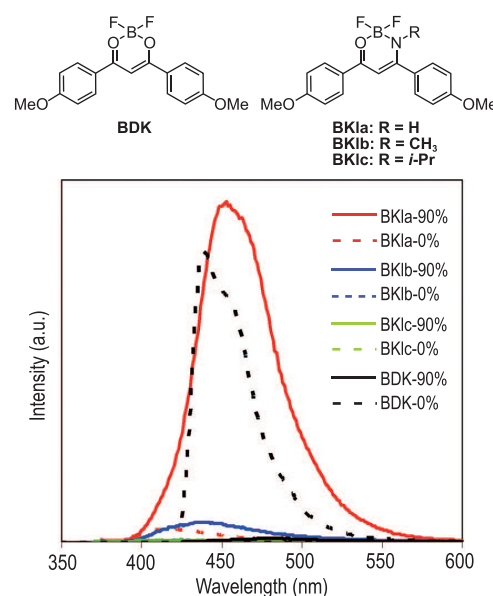


**Figure 4.** Chemical structures of $\beta$-diketonate and $\beta$-ketoiminate complexes and the dependency of photoluminescence spectra on the compositions of the solvents: THF (solid line) and THF/$H_2O$ (1 : 9) mixed solvent (dashed line). The concentration of each sample: $5.0 \times 10^{-5}$ M. Reprinted with permission from ref [26]. Copyright 2013 Wiley-VCH Verlag GmbH & Co. KGaA, Weinheim. Compounds were renamed.

luminescence and is expected to be utilized for pressure sensors and optical recording/memory devices [35–43]. The triads, BKM, containing two boron $\beta$-ketoiminates and the bithiophene linker with or without substituents at both ends, were synthesized (Fig. 5a) [44]. All the compounds showed similar electronic absorption and photoluminescence spectra in the solution states (Fig. 5b and c). Meanwhile, in the crystalline powder, the triads containing the smaller substituents, BKM-H(a) and BKM-F, provided yellow fluorescence. The compounds have relatively larger substituents, BKM-Cl, BKM-Br and BKM-I, exhibiting red fluorescence (Fig. 5d). Interestingly, mechanical grinding leads to hypsochromic and bathochromic shifts of the emission bands for the former group (BKM-H(a) and BKM-F) and the latter group (BKM-Cl, BKM-Br and BKM-I), respectively (Fig. 5e). The initial emission colors were recovered by heating the ground samples. From the results of powder X-ray diffraction and differential scanning calorimetry before and after the mechanical treatment, the grinding process increased the content of the amorphous domain of the samples. These observations suggested the following plausible mechanism of the contrary mechanochromic behavior depending on the kind of substituents (Fig. 5g): in the case of triads having smaller substituents, the molecules could interact with a
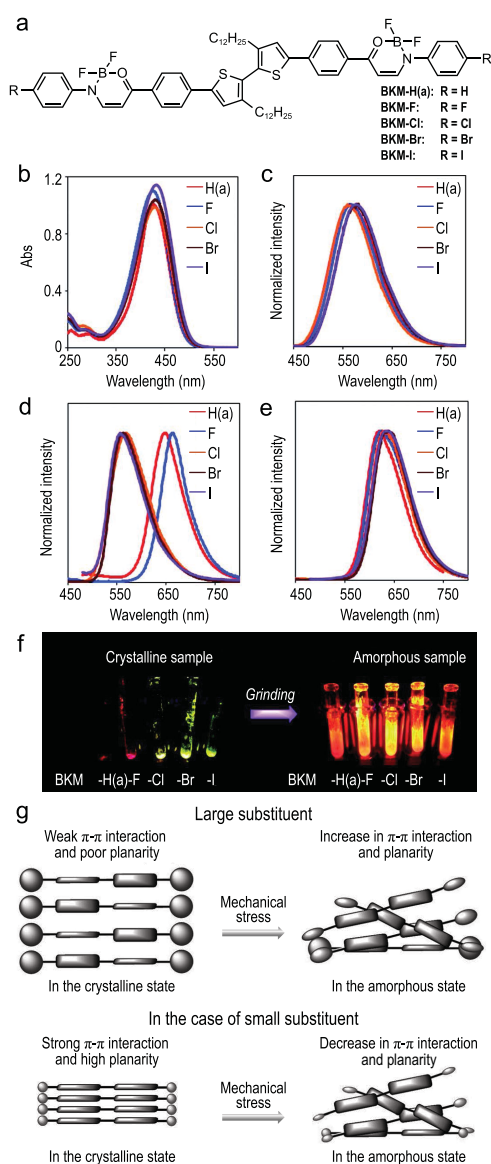
**Figure 5.** (a) Chemical structures of the triads composed of the boron $\beta$-ketoiminate core and the various substituents. (b) UV–Vis absorption, and (c) normalized photoluminescence spectra of the complexes in THF ($1 \times 10^{-5}$ M). Normalized photoluminescence spectra of the complexes in (d) the crystalline states, and (e) after grinding. (f) Photographs of the complexes in the crystalline (left) and amorphous (right) states under UV (365 nm) irradiation. (g) Illustration of a plausible mechanism of the effect of the substituents on the mechanochromic fluorescence. Reprinted with permission from ref [44]. Copyright 2015 Wiley-VCH Verlag GmbH & Co. KGaA, Weinheim. Compounds were renamed.

face-to-face motif and realize tight packing structures in the crystalline states. As a result, emission bands appeared in the relatively longer-wavelength regions in the initial crystalline states. By collapsing such tight packing, random molecular distributions should be obtained, resulting in the hypsochromic shifts. On the other hand, the steric hindrance of the larger substituents could disturb such a face-to-face stacking structure in the crystals. In the amorphous domains, $\pi$–$\pi$ interactions could be more frequently facilitated, leading to the bathochromic shifts. This is one example that offers environment-sensitive solid-state emission of AIE-active complexes.

## Boron $\beta$-diketiminate complexes

$\beta$-Diketiminate ligands, also known as $\beta$-diiminates, are the aza analogs of $\beta$-diketonate ligands as well as $\beta$-ketoiminate ligands. 'Ketimine' is the name of an imine analogous to a ketone, not to an aldehyde. '$\beta$-Ketoimine' is the name of an imine possessing a 'keto' group at the $\beta$ position of its imino group. Boron complexes of $\beta$-diketiminates are also likely to be AIE-active materials like $\beta$-ketoimine complexes, because both the oxygen atoms in $\beta$-diketonates are replaced by a nitrogen atom with a bulky and movable aryl group. Additionally, different types of substituents can be introduced independently into each aryl group of $\beta$-diketiminate ligands. Consequently, these ligands have been utilized in order to isolate the classes of unstable main-group and transition metal complexes composed of the group 13 elements, which had not been accessible using other bidentate ligands [45–54]. On the other hand, there have been a limited number of studies about the photophysical and electrochemical properties of these complexes, probably because the $\pi$-conjugation lengths of widely used $\beta$-diketiminate ligands are localized at the NCCCN and the corresponding complexes are usually colorless. However, it could be envisioned that $\beta$-diketiminate ligands would enable us to access functional optoelectronic materials and create possible applications of many kinds of metal complexes that have not been obtained by other ligands.

In an early study in 2008, it was reported that a boron $\beta$-diketiminate complex with an extended $\pi$-conjugation is fluorescent in the visible region. Importantly, it was clarified that the emission intensity of the complex is enhanced by aggregation, but the photoluminescence quantum yields in the solid state were not evaluated [55]. In later reports, it was reported that the luminescence quantum yields of the boron $\beta$-diketiminate complexes, BDKIa and BDKIb (Fig. 6a), were higher in the crystalline states ($\Phi_{PL} = 0.23$ for BDKIa and 0.11 for BDKIb) than those in the amorphous ($\Phi_{PL} = 0.02$ for both compounds) and solution states ($\Phi_{PL} < 0.01$ for both compounds) [56]. The crystalline aggregates can be obtained by reprecipitation from the mixture of acetonitrile solutions and water
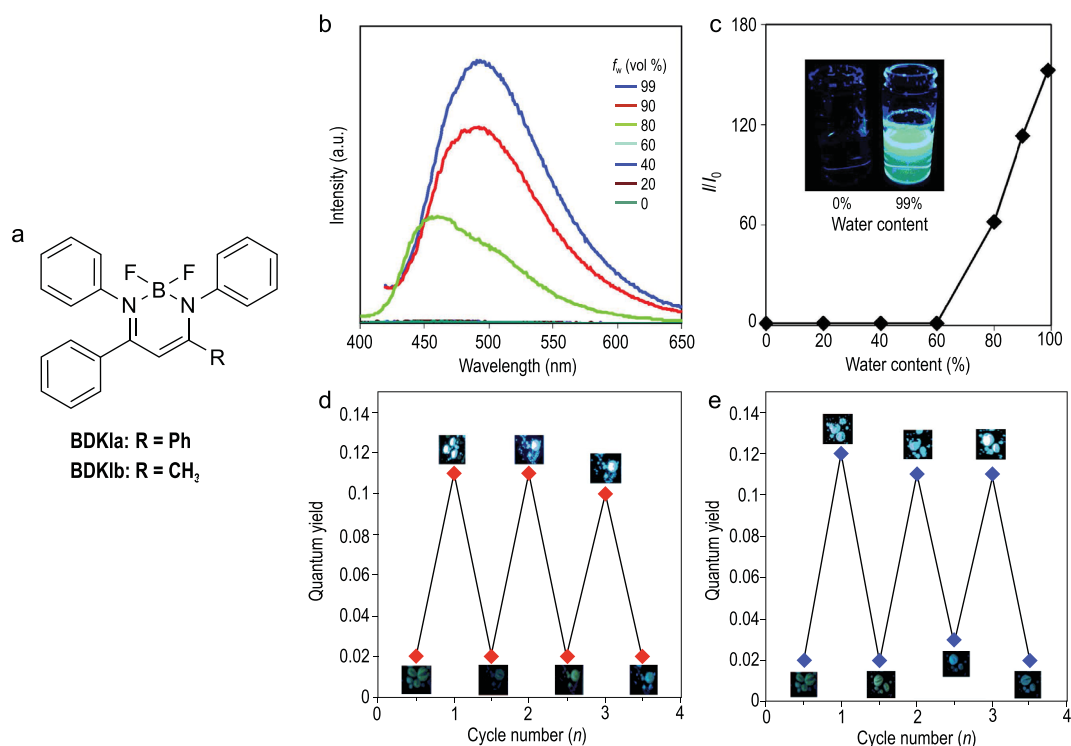
**Figure 6.** (a) Chemical structures of boron $\beta$-diketiminate complexes. (b) Photoluminescence spectra of BDKIa in the acetonitrile/H$_2$O mixture (5 $\times$ 10$^{-5}$ M) with various water contents ($f_w$). (c) Dependence of intensity ratio of BDKIa on $f_w$. Repeatability of the emission behavior of BDKIb between amorphous and crystalline states by (d) fuming–melt/quenching and (e) heating–melt/quenching cycles (see text for the detail). Reprinted with permission from ref [56]. Copyright 2014 Wiley-VCH Verlag GmbH & Co. KGaA, Weinheim. Compounds were renamed.

(Fig. 6b and c). The amorphous solids were prepared by rapid quenching of the melt samples (a melt/quenching process). The amorphous samples were converted to the crystalline sample by fuming the dichloromethane vapor for 30 minutes (a fuming process), or heating above the crystallization temperature (a heating process). Consequently, the crystalline and amorphous states of these complexes were interconverted repeatedly by means of the fuming–melt/quenching or heating–melt/quenching cycles (Fig. 6d and e). It was proposed that the packing structures in their crystalline states should play a critical role in the restriction of molecular vibrations and motions leading to non-radiative quenching paths. Since amorphous states are generally sparser than crystalline states, radiationless processes may be accessible enough to completely quench the excited energy without strong emission in the amorphous states. Therefore, the CIE property was observed in the boron $\beta$-diketiminates. Another group reported the AIE behavior of the similar boron complexes with fused ring structures at around the same time [57]. After these observations, the chemistry of the emission from boron $\beta$-diketiminates emerged [58–63].

Suzuki-Miyaura cross-coupling polycondensation between dihalogenated boron $\beta$-diketiminates and the corresponding comonomers successfully afforded AIE-active $\pi$-conjugated polymers [58]. The emission colors of the drop-cast films of the polymers are dependent on the electronic property of the substituent of the ligand (Fig. 7a and b). Complexes with an electron-donating substituent showed a bathochromic shift of their emission band compared to the non-substituted compounds. The electron-withdrawing substituents, on the other hand, hypsochromically shifted the luminescence spectra. Based on these observations, film-type luminescent sensors for acid-base [58] or redox [64] reactions were developed using this class of conjugated polymers. In the acid-base sensing system (Fig. 7c and d) [58], the emission properties were altered by acidification of the polymer films composed of the dimethylamino groups (P-NMe$_2$). Before treatment with the vapor of trifluoroacetic acid (TFA), the spin-coat films on quarts substrates of the polymer exhibited red emission. After the treatment of the films with the vapor of TFA, the emission color turned to yellow because the protonated ammonium groups acted as electron-withdrawing groups. Treatment with
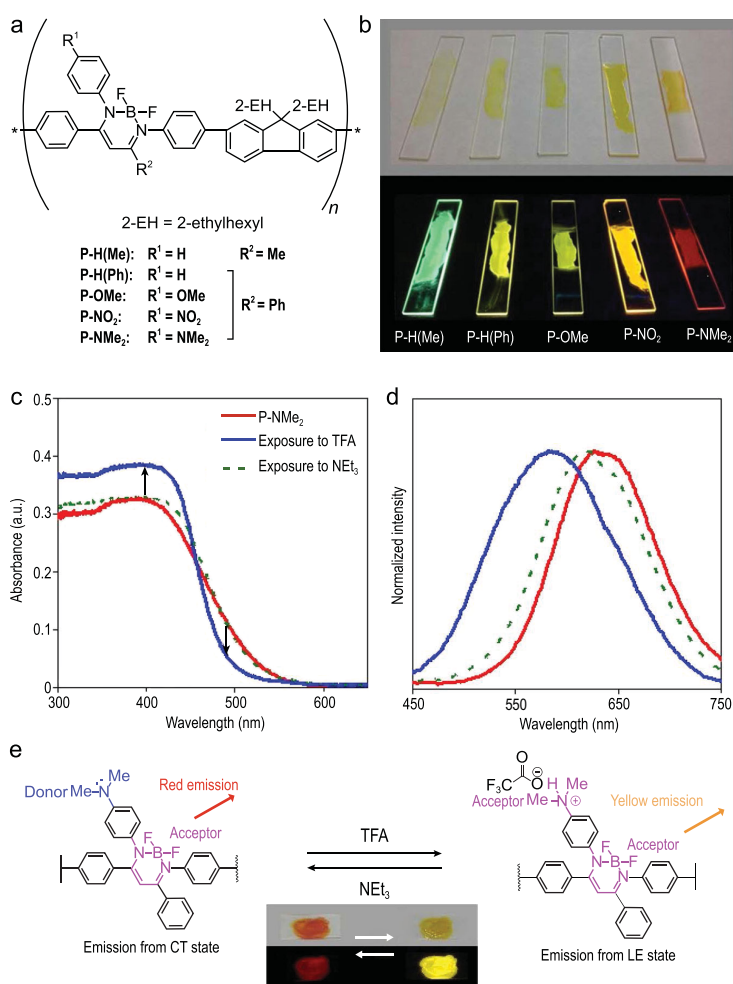
**Figure 7.** (a) Chemical structures of the conjugated polymers containing $\beta$-diketiminate complexes. (b) Photographs of the drop-cast films of the polymers formed on quartz substrates. (c) UV–Vis absorption and (d) photoluminescence spectra of P-NMe$_2$ before and after exposure to TFA and NEt$_3$ vapor in the thin-film state upon excitation at 391 nm. (e) Plausible mechanism of acid-base sensing. Reprinted with permission from ref [58]. Copyright 2014 American Chemical Society.

the triethylamine vapor recovered the initial red emission.

## BODIPY-based systems

Much effort has also been made to construct AIE-active systems based on BODIPY dyes, which are usually considered to be ineffective emitters in the solid states due to their planar structure as mentioned in the Introduction [65–69]. One of the incipient examples was reported in 2009 for donor–acceptor type luminogens (Fig. 8a) [65]. These molecules are composed of a diphenylamino group as an electron donor and a BODIPY moiety as an electron acceptor with one or two phenylene spacers. These compounds show a twisted intramolecular charge transfer (TICT) property. They ex-

hibit green emission derived from the locally-excited states in the low-polarity solvents, while the emission color changes to red, originating from the TICT state when the solvent polarity increases (Fig. 8b and c). The intensities of the red TICT emissions in tetrahydrofuran (THF)/water mixtures are strongly dependent on the contents of water ($f_w$). When $f_w$ is low (<60 vol%), the red emissions become negligible due to the very high hydrophilicity of water. In contrast, these molecules show their TICT emission when a large amount of water is added ($f_w >$ 70%) because the solutions cannot solvate the dyes and nanoaggregates are formed. In the case of BOD3 and BOD4, it is of interest to note that the emissions are enhanced compared to those in the pure THF solutions (Fig. 8d). Their intramolecular motions are likely to be restricted by the solidification.

Another exciting example was constructed with *meso*-trifluoromethyl-substituted BODIPY BOD-CF3 (Fig. 9a) [66]. The emission intensity of BOD-CF3 in the solution states is significantly lower ($\Phi_{PL} = 0.003$ in acetonitrile) than that of the methyl counterpart BOD-CH3 (Fig. 9b). Such weak luminescence may originate from the large structural difference between the $S_0$ and $S_1$ states resulting in the small Franck-Condon factor for the electronic transition. Surprisingly, the emission intensity of BOD-CF3 is enhanced as the volume fraction of water ($f_w$) of the acetonitrile/water mixtures increases. The colloidal suspension of the BOD-CF3 with 99% of $f_w$ shows sharpened absorption and emission spectra with a significantly small Stokes shift (51 cm$^{-1}$; 2 nm) compared to the acetonitrile solution (Fig. 9b). In sharp contrast, the aggregation causes the annihilation of the emission of BOD-CH3. The results of the single-crystal X-ray analysis revealed that the transition dipole moments of BOD-CF3 are aligned with 36°, while those of BOD-CH3 are aligned with 65° (Fig. 9c and d). These results clearly indicate that the formation of J-aggregation makes an efficiently emissive path in the BOD-CF3 aggregates, leading to a strong AIE effect. BOD-CH3, on the other hand, exhibits the H-type aggregation resulting in the optically dark states. Solid-state luminescent materials based on BODIPY dyes with such a J-aggregation character have attracted broad attention [68–74].

## Other four-coordinate boron complexes and origins of AIE properties

Most AIE-active molecules possess peripheral phenyl groups and rotative bonds, which probably accelerate non-radiative processes in the solution states, leading to emission annihilation. On the other hand, several boron complexes without such
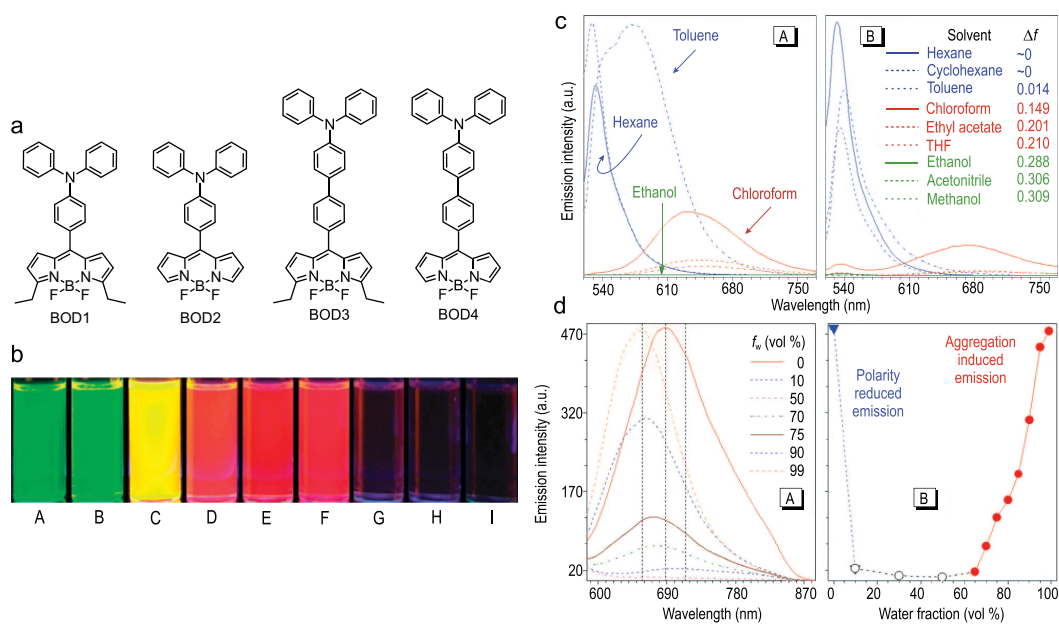
**Figure 8.** (a) Chemical structures of the BODIPY-based donor–acceptor luminogens. (b) Photographs of BOD1 under UV irradiation in various solvents (A: hexane; B: cyclohexane; C: toluene; D: chloroform; E: ethyl acetate; F: THF; G: ethanol; H: acetonitrile; I: methanol). (c) Photoluminescence spectra of (A) BOD1 and (B) BOD2 in the various solvents. (d) (A) Photoluminescence spectra and (B) emission intensities of BOD3 in THF/water mixtures with different water contents. Reprinted with permission from ref [65]. Copyright 2009 American Chemical Society.

structural features have shown AIE behavior [75]. As an interesting example, the photophysical properties of an azomethine complex, Az, are described here (Fig. 10a). Its optimized structures were estimated using a series of density functional theory (DFT) calculations in advance. It was implied that the complex would possess planar structure because of its fused structure (Fig. 10b). Indeed,



**Figure 9.** (a) Chemical structures of the *meso*-substituted BODIPYs. (b) Absorption and emission spectra of BOD-CF3 (left) and BOD-CH3 (right). Single-crystal structures of (c) BOD-CF3 and (d) BOD-CH3. Reproduced from ref [66] with permission from The Royal Society of Chemistry.

the structure determined from the analysis of the single-crystal X-ray diffraction of the synthesized complex is almost identical to the calculated structure. Interestingly, the optimized structure in the first singlet excited state ($S_1$) suggested drastic structural bending during structural relaxation (Fig. 10c). This structural bending should give rise to the localization of $\pi$-electrons and radiationless decay of the excited energy. Hence, it could be hypothesized that Az is likely to show the AIE property because aggregation would restrict the large relaxation process.

To evaluate the justification of our presumption, we synthesized Az [75]. Optical measurements revealed both the AIE and CIE properties of Az. A solution of Az shows a large Stokes shift at room temperature. This result indicates that a large structural relaxation should occur in the $S_1$ state. The fluorine atom protruding from the molecular plane seems to repel strong $\pi$–$\pi$ interactions. These data strongly encourage us to design a solid-state luminescence system based on boron complexes with such excited-state flexibility.

Additionally, it is of interest to note that temperature alteration causes unique mechanical movements and chromic behavior of the crystals of Az (Fig. 11). This complex was crystallized in the two distinct polymorphs, which exhibited green and yellow emission. Differential scanning calorimetry (DSC) clearly indicated that these two polymorphs
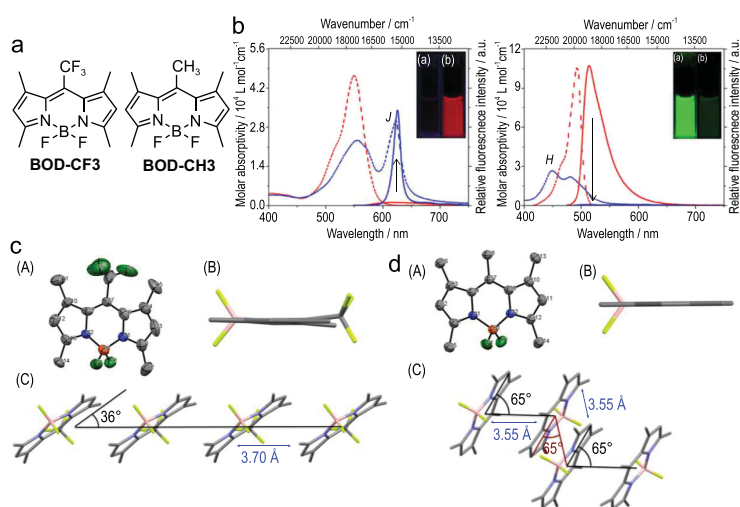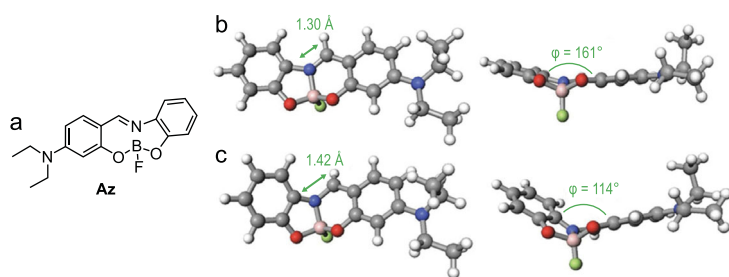
**Figure 10.** (a) The chemical structure of the azomethine complex Az. The optimized geometries of Az in (b) the $S_0$ and (c) the $S_1$ states. Optimization calculations were carried out at the B3LYP/6–311G** level for the ground state and the time-dependent B3LYP/6–311+G** level for the excited state. Reprinted with permission from ref [75]. Copyright 2017 Wiley-VCH Verlag GmbH & Co. KGaA, Weinheim.
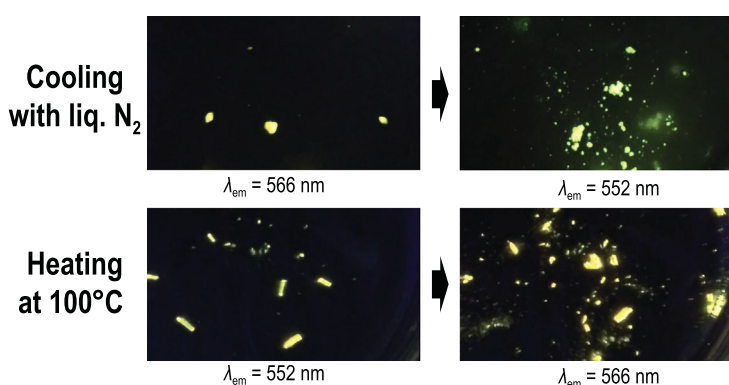


**Figure 11.** Photographs of the crystals of Az before/after cooling with (top) liquid nitrogen or (bottom) heating to 100°C under UV irradiation. Fracture of the crystals and emission color change can be observed. Reprinted with permission from ref [75]. Copyright 2017 Wiley-VCH Verlag GmbH & Co. KGaA.

thermally transformed each other. Surprisingly, mechanical movements such as hopping or fragmentation of the crystals were observed during heating and cooling. Such motion induced by thermal stimuli is known as the thermosalient effect. The results of powder X-ray diffraction analysis revealed that the crystal structure changes at the same time the thermosalient effect is observed. Moreover, this transition is also accompanied by the chromism of the appearance and the emission. The 'flexibility' of the boron complex might make its crystal sparser and tolerate the mechanical motions during the crystal transition.

Bending motions of four-coordinate boron complexes upon electronic excitation have been estimated in AIE-active boron difluorohydrazones [76]. A series of quantum calculations suggested that the bending motion of these molecules, named 'flip-flop', could lead the excited molecules to a conical intersection through which excitons non-radiatively quench. On the other hand, this class of complexes also possess rotative aryl groups. Other research has suggested that the restriction of the rotational mo-

tions of the peripheral aromatic ring could suppress the internal conversion of the excitons to the 'dark' $S_1$ state [77]. As shown above, the origins of the AIE and CIE properties are still not clear. Much more experimental and theoretical studies are required for a comprehensive understanding of these properties.

## OTHER GROUP 13 ELEMENTS

Studies of luminescent properties of four-coordinated compounds containing heavier group 13 elements are still rare. This is probably because the heavy group 13 elements such as Al and Ga prefer the five- or six-coordinated structures and the four-coordinated structures are usually unstable. Nevertheless, the construction of optical materials based on the heavy elements has been an attractive research topic since four-coordinated heavy elements promise to provide unique bonding and electronic nature [14,78–80]. In this section, we will provide a brief overview of aluminum- and gallium-containing AIE luminogens composed of $\beta$-diketiminate ligands. It is of interest to note that a few examples of AIE-active complexes [81] or metal–organic frameworks [82] have emerged. There is, of course, much room for development of photo-functional materials based on indium [83–85].

## Aluminum

The AIE and CIE nature of an aluminum-containing compound was reported for the dihydridoaluminum complex of a $\beta$-diketiminate ligand (Fig. 12a) [86]. This complex showed typical CIE behavior as well as a series of boron $\beta$-diketiminate complexes (Fig. 12b). From the results of DFT calculations, large structural relaxation, such as bending, was hardly observed. In addition, the phosphorescence quantum yield ($\sim$0.10) was considerably lower than the fluorescence quantum yield ($\sim$0.90) even at 77 K. Thus, we postulated that the non-radiative decay process in the solution state would be mainly attributed to internal conversion from $S_1$ to $S_0$. To estimate the contributions of each normal vibrational mode to the internal conversion, we calculated Huang–Rhys (HR) factors for the transition between $S_0$ and $S_1$ (Fig. 12c). The larger value of HR factors should indicate the larger contribution of the corresponding vibration to the radiationless quenching. The results of a series of DFT calculations suggested that the two types of vibrational modes, out-of-plane bending (Fig. 12d, left) and rotation of the peripheral aromatic rings (Fig. 12d, right), might play a pivotal role in the internal conversion process of the
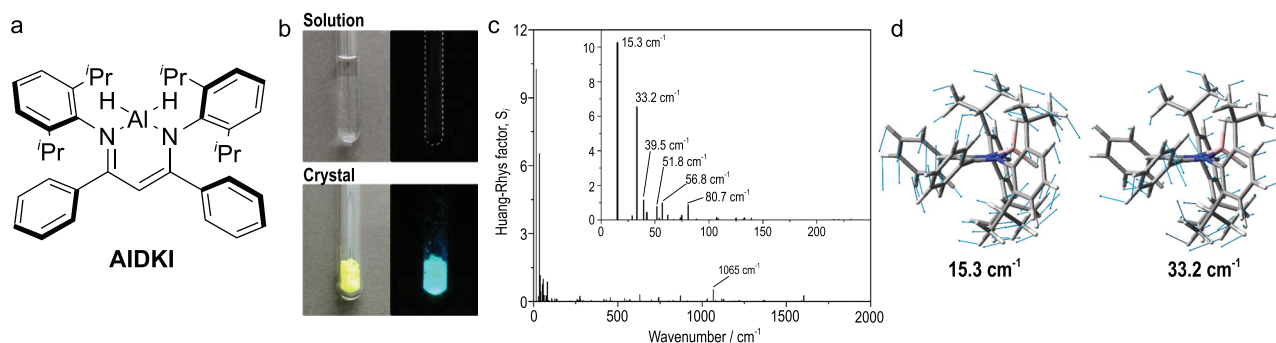
**Figure 12.** (a) The chemical structure of an aluminum $\beta$-diketiminate complex. (b) Photographs of the solution and crystalline states of AlDKI under natural light and UV (365 nm) irradiation. (c) Huang–Rhys factor, $S_i$, for each normal mode of AlDKI calculated for the $S_0$–$S_1$ transition. (Inset: low-frequency region.) Normal modes with relatively large HR factors ($S_i > 0.5$) are labeled with their wavenumber. (d) Displacement vectors attributed to the normal modes (left) $\omega_1$ (15.3 cm$^{-1}$) and (right) $\omega_3$ (33.2 cm$^{-1}$). Reprinted with permission from ref [86]. Copyright 2019 MDPI (Basel, Switzerland).
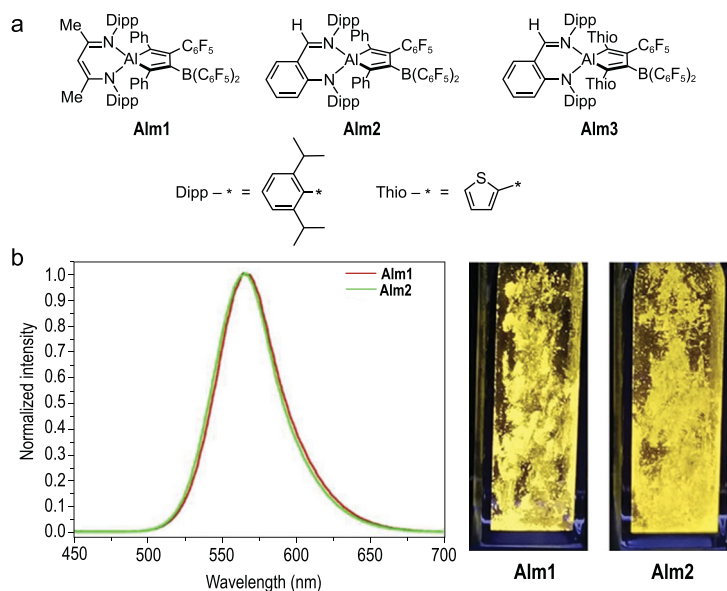


**Figure 13.** (a) Chemical structures of alumoles Alm1 and Alm2. (b) Normalized photo-luminescence spectra and photographs of the solids of Alm1 and Alm2 under UV-light irradiation 365 nm. Reprinted with permission from ref [87]. Copyright 2020 the authors. Published by Wiley-VCH Verlag GmbH & Co. KGaA. Compounds were renamed.

excited molecules. Importantly, this is the first report to assign the out-of-plane bending mode to a key factor of the AIE and CIE behavior of the complexes composed of the group 13 elements.

AIE-active aluminacyclopentadienes, named alumoles, have been reported recently. Alumoles can be regarded as the aluminum analog of siloles, which are important AIE-gens. Three ligand-stabilized alumoles, Alm1, Alm2 and Alm3 (Fig. 13a), were synthesized in the reaction between the dialkynyl complex $LAl(CCR)_2$ and tris(pentafluorophenyl)borane [87]. Interestingly, alumoles Alm1 and Alm2 showed typical AIE behavior. Their fluorescence emission bands in

benzene were very weak, whereas they exhibited bright yellow emissions in the solid state (Fig. 13b). The luminescence quantum yields of Alm1 and Alm2 were estimated to be 0.093% and 0.086%, respectively. In Alm1 and Alm2, there are six rings attached to the alumole core with two Ph, three $C_6F_5$ and one $AlN_2C_3$. These peripheral rings might be essential for AIE behavior. On the other hand, the alumole Alm3, which is the thienyl analog of Alm2, is hardly emissive in both solid and solution. The less planar central alumole ring might result in such annihilation of emission. The *N,N*-chelate ligand structures might also play a crucial role since such structures can be frequently found in the various AIE-active complexes. These promising results encourage us to develop novel AIE-gens constituted by the other group 13 heteroles, such as boroles and galloles.

## Gallium

Gallium has been employed as a central element of typical (semi-)metal complexes instead of boron. It can be envisioned that the larger ionic radius of gallium may induce sparse packing of gallium-based complexes in the crystalline states. Therefore, photophysical properties of gallium complexes could differ completely from the corresponding boron complexes. Indeed, the crystals of a gallium $\beta$-diketiminate complex (GaDKI, Fig. 14a) exhibited more efficient photoluminescence than the corresponding boron complex [59]. This enhancement of the luminescence might result from the relatively weak intermolecular electronic interactions in the crystalline state of the gallium complex. It is of interest to note that solvent-vapor annealing brings about the emission-color change accompanied by the crystal–crystal phase transition (Fig. 14b and c). When the crystalline powder is exposed to the
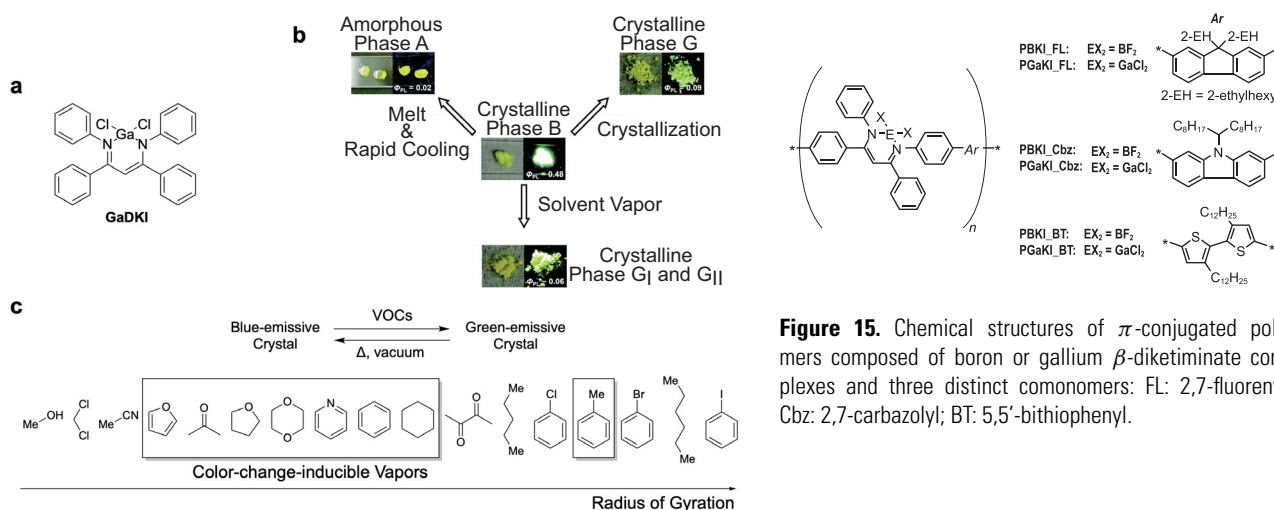
**Figure 14.** (a) The chemical structure of a gallium $\beta$-diketiminate complex. (b) Photographs of the complexes in each state and the stimuli-responsive behavior. Reproduced from ref [59] with permission from The Royal Society of Chemistry. (c) Schematic representation of the vapochromic luminescence. Compound was renamed.



**Figure 15.** Chemical structures of $\pi$-conjugated polymers composed of boron or gallium $\beta$-diketiminate complexes and three distinct comonomers: FL: 2,7-fluorenyl; Cbz: 2,7-carbazolyl; BT: 5,5′-bithiophenyl.

**Table 1.** Photophysical and electronic properties of the polymers.

| | $\lambda_{abs}^{solution}$/nm | $\lambda_{PL}^{film}$ nm | $\Phi_{PL}^{solution}$ $\Phi_{PL}^{film}$ | $E_{HOMO}$/eV[a] | $E_{LUMO}$/eV[a] |
|---|---|---|---|---|---|
| PBKI_FL | 399 | 545 | <0.01 0.07 | −6.27 | −3.53 |
| PBKI_Cbz | 397 | 552 | <0.01 0.07 | −6.18 | −3.44 |
| PBKI_BT | 404 | 575 | <0.01 0.07 | −6.10 | −3.45 |
| PGaKI_FL | 411 | 575 | <0.01 0.05 | −6.19 | −3.60 |
| PGaKI_Cbz | 410 | 573 | <0.01 0.05 | −6.15 | −3.54 |
| PGaKI_BT | 420 | 601 | <0.01 0.03 | −6.08 | −3.54 |

[a]Calculated from the results of cyclic voltammetry and optical band gap ($E_g^{opt}$) with the following empirical formula: $E_{HOMO}$/eV $= E_{LUMO}$/eV $- E_g^{opt}$/eV, $E_{LUMO}$/eV $= -E_{red}$/eV $- 4.80$.

vapor of specific volatile organic compounds (VOCs), the color of fluorescence changes rapidly from blue to green. Surprisingly, only the VOCs with a limited range of radius of gyration (1.75–2.02 Å) induce such chromic fluorescence with crystal–crystal transition. The other evaluated parameters of the VOCs, vapor pressure and dipole moment, are independent of whether the chromism occurs or not. Such a transition might be realized by the introduction of flexibility in the crystal originating from the weak gallium–nitrogen coordination. With regard to these results, $\beta$-diketiminate complexes have attracted attention for developing

functional solid-state luminescent materials. Additionally, it is worth noting that GaDKI is the first example of the AIE- and CIE-active gallium complex.

$\pi$-Conjugated polymers containing gallium $\beta$-diketiminates, PGaKI_FL, PGaKI_Cbz and PGaKI_BT (Fig. 15), were synthesized through the post-complexation methodology with the corresponding polymeric ligands [61]. Photophysical, electrochemical and theoretical studies suggested that the lowest unoccupied molecular orbitals (LUMOs) of the gallium-containing polymers should be lying at lower energy levels than those of the corresponding boron polymers, PBKI_FL, PBKI_Cbz and PBKI_BT (Table 1). Meanwhile, their highest occupied molecular orbitals (HOMOs) stayed at a similar level. As a result, the gallium polymers exhibited the AIE behavior in a lower energy region than the boron polymers. It was also implied that the synthetic approach through polymeric ligands should provide a versatile way to access functional polymers composed of complexes with other heavy elements.

## CONCLUSION

Recent advances in the development of AIE-active complexes composed of the group 13 elements are reviewed. Various types of stimuli-responsive chromic materials, as well as solid-state emissive molecules, have become accessible by AIE-active element blocks. Additionally, it is anticipated that 'flexibility' of boron complexes at electronically excited states is likely to be one of the key factors in the AIE property of the complexes. In order to detect tiny stimuli and slight environmental changes, we still require enhancement of sensitivity in optical sensors. Therefore, AIE-active element blocks based on the group 13 elements with novel

chemical structures would be a scaffold for designing and constructing advanced sensing materials to meet these demands. Furthermore, the number of examples of AIE- and CIE-active compounds composed of aluminum or gallium has been gradually increasing. In addition, a few examples of AIE-active systems based on indium complexes have emerged. Further development of these sprouting studies must enable the heavier elements to show their stuff as next-generation functional optoelectronic materials.

## FUNDING

*Conflict of interest statement.* None declared.

## REFERENCES

1. Becker HD. Unimolecular photochemistry of anthracenes. *Chem Rev* 1993; **93**: 145–72.

2. Winnik FM. Photophysics of preassociated pyrenes in aqueous polymer solutions and in other organized media. *Chem Rev* 1993; **93**: 587–614.

3. Feng X, Hu J-Y and Redshaw C *et al.* Functionalization of pyrene to prepare luminescent materials—typical examples of synthetic methodology. *Chem Eur J* 2016; **22**: 11898–916.

4. Hofer LJE, Grabenstetter RJ and Wiig EO. The fluorescence of cyanine and related dyes in the monomeric state 1. *J Am Chem Soc* 1950; **72**: 203–9.

5. Pansare VJ, Hejazi S and Faenza WJ *et al.* Review of long-wavelength optical and NIR imaging materials: contrast agents, fluorophores, and multifunctional nano carriers. *Chem Mater* 2012; **24**: 812–27.

6. Yin J, Kwon Y and Kim D *et al.* Cyanine-based fluorescent probe for highly selective detection of glutathione in cell cultures and live mouse tissues. *J Am Chem Soc* 2014; **136**: 5351–8.

7. Cao D, Liu Z and Verwilst P *et al.* Coumarin-based small-molecule fluorescent chemosensors. *Chem Rev* 2019; **119**: 10403–519.

8. Ziessel R, Ulrich G and Harriman A. The chemistry of Bodipy: a new *El Dorado* for fluorescence tools. *New J Chem* 2007; **31**: 496–501.

9. Loudet A and Burgess K. BODIPY dyes and their derivatives: syntheses and spectroscopic properties. *Chem Rev* 2007; **107**: 4891–932.

10. Hong Y, Lam JWY and Tang BZ. Aggregation-induced emission. *Chem Soc Rev* 2011; **40**: 5361–88.

11. Mei J, Leung NLC and Kwok RTK *et al.* Aggregation-induced emission: together we shine, united we soar! *Chem Rev* 2015; **115**: 11718–940.

12. Ochi J, Tanaka K and Chujo Y. Recent progress in the development of solid-state luminescent *o*-carboranes with stimuli responsivity. *Angew Chem Int Ed* 2020; **59**: 9841–55.

13. Chujo Y and Tanaka K. New polymeric materials based on element-blocks. *Bull Chem Soc Jpn* 2015; **88**: 633–43.

14. Gon M, Tanaka K and Chujo Y. Recent progress in the development of advanced element-block materials. *Polym J* 2017; **50**: 13–7.

15. Gon M, Tanaka K and Chujo Y. Concept of excitation-driven boron complexes and their applications for functional luminescent materials. *Bull Chem Soc Jpn* 2019; **92**: 7–18.

16. Mukherjee S and Thilagar P. Boron clusters in luminescent materials. *Chem Commun* 2016; **52**: 1070–93.

17. Frath D, Massue J and Ulrich G *et al.* Luminescent materials: locking $\pi$-conjugated and heterocyclic ligands with boron(III). *Angew Chem Int Ed* 2014; **53**: 2290–310.

18. Zhang G, Lu J and Sabat M *et al.* Polymorphism and reversible mechanochromic luminescence for solid-state difluoroboron avobenzone. *J Am Chem Soc* 2010; **132**: 2160–2.

19. Wang L, Zhang Z and Cheng X *et al.* Red emissive diaryl-boron diketonate crystals: aggregation-induced color change and amplified spontaneous emission. *J Mater Chem C* 2015; **3**: 499–505.

20. DeRosa CA, Samonina-Kosicka J and Fan Z *et al.* Oxygen sensing difluoroboron dinaphthoylmethane polylactide. *Macromolecules* 2015; **48**: 2967–77.

21. Mo H, Tsuchiya Y and Geng Y *et al.* Color tuning of avobenzone boron difluoride as an emitter to achieve full-color emission. *Adv Funct Mater* 2016; **26**: 6703–10.

22. DeRosa CA, Hiroto S and Fraser CL. Amplified heavy-atom free phosphorescence from *meta*-dimethoxy difluoroboron $\beta$-diketonate charge-transfer materials. *J Phys Chem C* 2019; **123**: 20488–96.

23. Galer P, Korošec RC and Vidmar M *et al.* Crystal structures and emission properties of the BF$_2$ complex 1-phenyl-3-(3,5-dimethoxyphenyl)-propane-1,3-dione: multiple chromisms, aggregation- or crystallization-induced emission, and the self-assembly effect. *J Am Chem Soc* 2014; **136**: 7383–94.

24. Morris WA, Kolpaczynska M and Fraser CL. Effects of $\alpha$-substitution on mechanochromic luminescence and aggregation-induced emission of difluoroboron $\beta$-diketonate dyes. *J Phys Chem C* 2016; **120**: 22539–48.

25. Kubota Y, Tanaka S and Funabiki K *et al.* Synthesis and fluorescence properties of thiazole–boron complexes bearing a $\beta$-ketoiminate ligand. *Org Lett* 2012; **14**: 4682–5.

26. Yoshii R, Nagai A and Tanaka K *et al.* Highly emissive boron ketoiminate derivatives as a new class of aggregation-induced emission fluorophores. *Chem Eur J* 2013; **19**: 4506–12.

27. Yoshii R, Nagai A and Tanaka K *et al.* Boron-ketoiminate-based polymers: fine-tuning of the emission color and expression of strong emission both in the solution and film states. *Macromol Rapid Commun* 2014; **35**: 1315–9.

28. Yoshii R, Tanaka K and Chujo Y. Conjugated polymers based on tautomeric units: regulation of main-chain conjugation and expression of aggregation-induced emission property via boron-complexation. *Macromolecules* 2014; **47**: 2268–78.

29. Suenaga K, Yoshii R and Tanaka K *et al.* Sponge-type emissive chemosensors for the protein detection based on boron ketoiminate-modifying hydrogels with aggregation-induced blueshift emission property. *Macromol Chem Phys* 2016; **217**: 414–21.

30. Suenaga K, Tanaka K and Chujo Y. Heat-resistant mechanoluminescent chromism of the hybrid molecule based on boron ketoiminate modified octasubstituted polyhedral oligomeric silsesquioxane. *Chem Eur J* 2017; **23**: 1409–14.

31. Zhou L, Xu D and Gao H *et al.* Triphenylamine functionalized $\beta$-ketoiminate boron complex exhibiting aggregation-induced emission and mechanofluorochromism. *Dyes Pigm* 2017; **137**: 200–7.

32. Fedorenko EV, Mirochnik AG and Beloliptsev AY *et al.* Design, synthesis, and crystallization-induced emission of boron difluorides $\beta$-ketoiminates. *ChemPlusChem* 2018; **83**: 117–27.

33. Suenaga K, Uemura K and Tanaka K *et al.* Stimuli-responsive luminochromic polymers consisting of multi-state emissive fused boron ketoiminate. *Polym Chem* 2020; **11**: 1127–33.

34. Huheey JE, Keiter EA and Keiter RL. *Inorganic Chemistry: Principles of Structure and Reactivity*, 4th edn. New York: Harper Collins College Publishers, 1993.

35. Chi Z, Zhang X and Xu B *et al.* Recent advances in organic mechanofluorochromic materials. *Chem Soc Rev* 2012; **41**: 3878–96.

36. Wiggins KM, Brantley JN and Bielawski CW. Methods for activating and characterizing mechanically responsive polymers. *Chem Soc Rev* 2013; **42**: 7130–47.

37. McConnell AJ, Wood CS and Neelakandan PP *et al.* Stimuli-responsive metal–ligand assemblies. *Chem Rev* 2015; **115**: 7729–93.

38. Xue P, Ding J and Wang P *et al.* Recent progress in the mechanochromism of phosphorescent organic molecules and metal complexes. *J Mater Chem C* 2016; **4**: 6688–706.

39. Mukherjee S and Thilagar P. Stimuli and shape responsive 'boron-containing' luminescent organic materials. *J Mater Chem C* 2016; **4**: 2647–62.

40. Wang C and Li Z. Molecular conformation and packing: their critical roles in the emission performance of mechanochromic fluorescence materials. *Mater Chem Front* 2017; **1**: 2174–94.

41. Chen P-Z, Niu L-Y and Chen Y-Z *et al.* Difluoroboron $\beta$-diketonate dyes: spectroscopic properties and applications. *Coord Chem Rev* 2017; **350**: 196–216.

42. Yang Z, Chi Z and Mao Z *et al.* Recent advances in mechano-responsive luminescence of tetraphenylethylene derivatives with aggregation-induced emission properties. *Mater Chem Front* 2018; **2**: 861–90.

43. Mellerup SK and Wang S. Boron-based stimuli responsive materials. *Chem Soc Rev* 2019; **48**: 3537–49.

44. Yoshii R, Suenaga K and Tanaka K *et al.* Mechanofluorochromic materials based on aggregation-induced emission-active boron ketoiminates: regulation of the direction of the emission color changes. *Chem Eur J* 2015; **21**: 7231–7.

45. Bourget-Merle L, Lappert MF and Severn JR. The chemistry of $\beta$-diketiminatometal complexes. *Chem Rev* 2002; **102**: 3031–66.

46. Camp C and Arnold J. On the non-innocence of 'nacnacs': ligand-based reactivity in $\beta$-diketiminate supported coordination compounds. *Dalton Trans* 2016; **45**: 14462–98.

47. Piers WE and Emslie DJH. Non-cyclopentadienyl ancillaries in organogroup 3 metal chemistry: a fine balance in ligand design. *Coord Chem Rev* 2002; **233–4**: 131–55.

48. Roesky HW, Singh S and Jancik V *et al.* A paradigm change in assembling OH functionalities on metal centers. *Acc Chem Res* 2004; **37**: 969–81.

49. Mindiola DJ. Oxidatively induced abstraction reactions. A synthetic approach to low-coordinate and reactive early transition metal complexes containing metal—ligand multiple bonds. *Acc Chem Res* 2006; **39**: 813–21.

50. Cramer CJ and Tolman WB. Mononuclear Cu–$O_2$ complexes: geometries, spectroscopic properties, electronic structures, and reactivity. *Acc Chem Res* 2007; **40**: 601–8.

51. Holland PL. Electronic structure and reactivity of three-coordinate iron complexes. *Acc Chem Res* 2008; **41**: 905–14.

52. Mindiola DJ. Nacnac …Are you still there? The evolution of $\beta$-diketiminate complexes of nickel. *Angew Chem Int Ed* 2009; **48**: 6198–200.

53. Tsai YC. The chemistry of univalent metal $\beta$-diketiminates. *Coord Chem Rev* 2012; **256**: 722–58.

54. Chen C, Bellows SM and Holland PL. Tuning steric and electronic effects in transition-metal $\beta$-diketiminate complexes. *Dalton Trans* 2015; **44**: 16654–70.

55. Macedo FP, Gwengo C and Lindeman SV *et al.* $\beta$-Diketonate, $\beta$-ketoiminate, and $\beta$-diiminate complexes of difluoroboron. *Eur J Inorg Chem* 2008; **2008**: 3200–11.

56. Yoshii R, Hirose A and Tanaka K *et al.* Boron diiminate with aggregation-induced emission and crystallization-induced emission-enhancement characteristics. *Chem Eur J* 2014; **20**: 8320–4.

57. Perumal K, Garg JA and Blacque O *et al.* $\beta$-Iminoenamine-$BF_2$ complexes: aggregation-induced emission and pronounced effects of aliphatic rings on radiationless deactivation. *Chem Asian J* 2012; **7**: 2670–7.

58. Yoshii R, Hirose A and Tanaka K *et al.* Functionalization of boron diiminates with unique optical properties: multicolor tuning of crystallization-induced emission and introduction into the main chain of conjugated polymers. *J Am Chem Soc* 2014; **136**: 18131–9.

59. Ito S, Hirose A and Yamaguchi M *et al.* Size-discrimination of volatile organic compounds utilizing gallium diiminate by luminescent chromism of crystallization-induced emission via encapsulation-triggered crystal–crystal transition. *J Mater Chem C* 2016; **4**: 5564–71.

60. Yamaguchi M, Ito S and Hirose A *et al.* Modulation of sensitivity to mechanical stimulus in mechanofluorochromic properties by altering substituent positions in solid-state emissive diiodo boron diiminates. *J Mater Chem C* 2016; **4**: 5314–9.

61. Ito S, Hirose A and Yamaguchi M *et al.* Synthesis of aggregation-induced emission-active conjugated polymers composed of group 13 diiminate complexes with tunable energy levels via alteration of central element. *Polymers* 2017; **9**: 68.

62. Yamaguchi M, Ito S and Hirose A *et al.* Control of aggregation-induced emission versus fluorescence aggregation-caused quenching by bond existence at a single site in boron pyridinoiminate complexes. *Mater Chem Front* 2017; **1**: 1573–9.

63. Tanaka K and Chujo Y. Luminescent color tuning with polymer films composed of boron diiminate conjugated copolymers by changing the connection points to comonomers. *Polym Chem* 2018; **9**: 1942–6.

64. Hirose A, Tanaka K and Yoshii R *et al.* Film-type chemosensors based on boron diiminate polymers having oxidation-induced emission properties. *Polym Chem* 2015; **6**: 5590–5.

65. Hu R, Lager E and Aguilar-Aguilar A *et al.* Twisted intramolecular charge transfer and aggregation-induced emission of BODIPY derivatives. *J Phys Chem C* 2009; **113**: 15845–53.

66. Choi S, Bouffard J and Kim Y. Aggregation-induced emission enhancement of a *meso*-trifluoromethyl BODIPY via J-aggregation. *Chem Sci* 2013; **5**: 751–5.

67. Chua MH, Ni Y and Garai M *et al.* Towards *meso*-ester BODIPYs with aggregation-induced emission properties: the effect of substitution positions. *Chem Asian J* 2015; **10**: 1631–4.

68. Mukherjee S and Thilagar P. Fine-tuning dual emission and aggregation-induced emission switching in NPI-BODIPY dyads. *Chem Eur J* 2014; **20**: 9052–62.

69. Kumar PPP, Yadav P and Shanavas A *et al.* Aggregation enhances luminescence and photosensitization properties of a hexaiodo-BODIPY. *Mater Chem Front* 2020; **4**: 965–72.

70. Bergström F, Mikhalyov I and Hägglöf P *et al.* Dimers of dipyrrometheneboron difluoride (BODIPY) with light spectroscopic applications in chemistry and biology. *J Am Chem Soc* 2002; **124**: 196–204.

71. Kim S, Bouffard J and Kim Y. Tailoring the solid–state fluorescence emission of BODIPY dyes by *meso* substitution. *Chem Eur J* 2015; **21**: 17459–65.

72. Spies C, Huynh A-M and Huch V *et al.* Correlation between crystal habit and luminescence properties of 4,4-difluoro-1,3-dimethyl-4-bora-3a,4a-diaza-*s*-indacene, an asymmetric BODIPY dye. *J Phys Chem C* 2013; **117**: 18163–9.

73. Vu TT, Dvorko M and Schmidt EY *et al.* Understanding the spectroscopic properties and aggregation process of a new emitting boron dipyrromethene (BODIPY). *J Phys Chem C* 2013; **117**: 5373–85.

74. Okada D, Nakamura T and Braam D *et al.* Color-tunable resonant photoluminescence and cavity-mediated multistep energy transfer cascade. *ACS Nano* 2016; **10**: 7058–63.

75. Ohtani S, Gon M and Tanaka K *et al.* A flexible, fused, azomethine-boron complex: thermochromic luminescence and thermosalient behavior in structural transitions between crystalline polymorphs. *Chem Eur J* 2017; **23**: 11827–33.

76. Zhou P, Li P and Zhao Y *et al.* Restriction of flip-flop motion as a mechanism for aggregation-induced emission. *J Phys Chem Lett* 2019; **10**: 6929–35.

77. Qian H, Cousins ME and Horak EH *et al.* Suppression of Kasha's rule as a mechanism for fluorescent molecular rotors and aggregation-induced emission. *Nat Chem* 2017; **9**: 83–7.

78. Manners I. Polymers and the periodic table: recent developments in inorganic polymer science. *Angew Chem Int Ed* 1996; **35**: 1602–21.

79. Priegert AM, Rawe BW and Serin SC *et al.* Polymers and the p-block elements. *Chem Soc Rev* 2016; **45**: 922–53.

80. Vidal F and Jäkle F. Functional polymeric materials based on main-group elements. *Angew Chem Int Ed* 2019; **58**: 5846–70.

81. Du X, Fan R and Wang X *et al.* Combined effect of hydrogen bonding and $\pi \cdots \pi$ stacking interactions in the assembly of indium(III) metal–organic materials: structure-directing and aggregation-induced emission behavior. *Cryst Growth Des* 2015; **15**: 2402–12.

82. Zhou X-S, Fan R-Q and Du X *et al.* Key effect of robust $\pi \cdots \pi$ stacking on AIE performance for supramolecular indium(III)–organic assemblies and application in PMMA-doped hybrid material. *Inorg Chem Commun* 2018; **90**: 39–44.

83. Lee S, Shin N and Kwak S *et al.* Intriguing indium-salen complexes as multicolor luminophores. *Inorg Chem* 2017; **56**: 2621–6.

84. Hyun K, Jin H and Woo WH *et al.* Systematic design of indium-based luminophores with color-tunable emission via combined manipulation of HOMO and LUMO levels. *Dyes Pigm* 2018; **158**: 285–94.

85. Kwak S, Kwon H and Lee J *et al.* Salen-indium/triarylborane triads: synthesis and ratiometric emission-colour changes by fluoride ion binding. *Dalton Trans* 2018; **47**: 5310–7.

86. Ito S, Tanaka K and Chujo Y. Characterization and photophysical properties of a luminescent aluminum hydride complex supported by a $\beta$-diketiminate ligand. *Inorganics* 2019; **7**: 100.

87. Li J, Wu P and Jiang W *et al.* An unusual and facile synthetic route to alumoles. *Angew Chem Int Ed* 2020; **59**: 10027–31.